Journal of Ambient Intelligence and Humanized Computing (2022) 13:3619–3631
https://doi.org/10.1007/s12652-020-02024-9

ORIGINAL RESEARCH

Effective epileptic seizure detection based on the event-driven processing and machine learning for mobile healthcare

Saeed Mian Qaisar[1] · **Abdulhamit Subasi**[1]

Received: 9 November 2019 / Accepted: 23 April 2020 / Published online: 4 May 2020

Abstract
Mobile healthcare is a promising approach. It is realized by using the biomedical implants that are connected to the cloud. A framework for the precise and effective diagnosis of epileptic seizures is designed in this context. To achieve real-time compression and effective signal processing and transmission, it uses an intelligent event-driven electroencephalogram (EEG) signal acquisition. Experimental results show that grace of the event-driven nature an overall 3.3 fold compression and transmission bandwidth usage reduction is achieved by the devised method compared to the conventional counterparts. It promises a notable decrease in the post analysis and classification processing activity. The system performance is studied by using a standard three class EEG epileptic seizure dataset. The highest classification accuracy of 97.5% is secured for a mono-class. The best average classification accuracy of 96.4% is attained for three-classes. Comparison of the system with classical equivalents is made. Results demonstrate more than threefold and sevenfold of outperformance respectively in terms of compression gain and processing efficiency while confirming a comparable classification precision.

Keywords Electroencephalogram · Epileptic seizure diagnosis · Event-driven processing · Compression · AR burg features extraction · Machine learning · Biomedical implants · Mobile healthcare

1 Introduction

1.1 Background

According to the World Health Organization (WHO), millions of people are suffering from epilepsy worldwide (Saxena and Li 2017). Epilepsy is a neurodegenerative disorder whose crucial sign is the incidence of epileptic seizures. A temporary electrical disturbance of the brain that interrupts the electrical communication between neurons causes the epileptic seizures. This might happen as a partial seizure or generalized seizures (Pitkänen et al. 2017).

Serious damages could happen to patients with uncontrolled epilepsy such as physical injuries and deaths (Devinsky et al. 2017). In spite of pharmacological treatment, at least 20 percent of all patients with epilepsy retain seizures due to the treatment inefficacy. It is the motivation for several researchers to invent new methods of the epileptic seizure prevention such as chronic vagal nerve stimulation, drug injection and patient alarming (Osorio and Frei 2017; Schmidt and Sillanpää 2016). Such a seizure prevention system timely alerts patient and prevents patients from taking ineffective amount of medicine (Schmidt and Sillanpää 2016). Hence, an accurate and automatic detection of seizures can not only augment the effectiveness of epileptologist diagnosis but can also enhance the life quality of intended patients.

Detection of epileptic conditions is realizable by analyzing the EEG signals (Martinez-del-Rincon et al. 2017). In this framework, diverse wearable EEG devices have been proposed (Gu et al. 2018; Elger and Hoppe 2018). However, EEG based seizure detection is not straightforward. It includes huge amounts of data to tackle as the EEG signal recordings are collected from multiple scalp electrodes (Schröder and Ombao 2019; Tawfik et al. 2016). Additionally, the interferences and physiological artifacts alter the EEG signal by decreasing the effectiveness of the post features extraction and classification (Gupta and Pachori 2019). To overcome these deficiencies numerous signal processing

✉ Saeed Mian Qaisar
sqaisar@effatuniversity.edu.sa

Abdulhamit Subasi
absubasi@effatuniversity.edu.sa

[1] College of Engineering, Effat University, Jeddah 22332, Saudi Arabia

techniques have been presented (Gupta and Pachori 2019). Several techniques have been implemented for preprocessing of the EEG signals such as Kalman filtering (Baskar and Karthikeyan 2019), orthogonal wavelet filters (Sharma et al. 2018), Adaptive filtering (Correa et al. 2019), and principal component analysis (Chen et al. 2017).

The EEG signals are processed and analyzed with sophisticated signal processing methods in order to effectively identify the epileptic seizures (Gupta and Pachori 2019; Baskar and Karthikeyan 2019; Chen et al. 2017). The Discrete Wavelet Transform (DWT), Wavelet Packet Decomposition (WPD), and Autoregressive (AR) Burg are the frequently employed tools for the EEG features extraction (Chen et al. 2017; Zhang et al. 2017b).

The discriminative characteristics, obtained with the feature extraction process are employed for automatic diagnosis of the epileptic seizures. Numerous data mining techniques have been presented for the EEG signals classification (Zazzaro et al. 2019). Certain key EEG classifications approaches are the neural networks, Support Vector Machines (SVMs), k-means clustering, the k-nearest neighbor (k-NN), and the Fuzzy logic (Zazzaro et al. 2019; Subasi 2019).

1.2 Research motivation

The effective epilepsy treatment can be realized with a timely detection of epileptic seizures. Precise and timely notification of abnormal conditions to the epileptologists is vital in smart healthcare monitoring and management. In this framework, the mobile healthcare systems can proficiently expand the management of chronic disorders and emergencies (Elger and Hoppe 2018; Hosseini et al. 2016; Bayrakdar 2019a, b). Hence, patients with epilepsy require a continuous monitoring. Wearable EEG sensor is one of the best tools in this framework (Gu et al. 2018). Smartphones can acquire the information from the EEG sensors and transmit findings to a monitoring center (Gu et al. 2018). Moreover, in case of emergency the mobile application can be employed to automatically call the emergency center or clinician with details of patient's GPS location (Hosseini et al. 2016).

The design of smart EEG wearables is revitalizing because of strict restrictions on size, weight, and power consumption. Self-powered smart sensors are generally preferred in such circumstances since they enable continuous acquisition of multichannel EEG signals without producing embarrassments to the patient. The substantial saving of power in a wireless EEG device is only possible by minimizing the usage of wireless transceiver, i.e. transmitting valuable data is preferred over the raw data (Gu et al. 2018; Elger and Hoppe 2018). In order to achieve this, many studies are carried out on the EEG signal compression (Qaisar and Subasi 2019a; Zeng et al. 2016) non-uniform sampling (Mesin 2016) and event-driven data acquisition (Qaisar 2018; Qaisar and Subasi 2019b; Zhang et al. 2017a; Antony et al. 2018; Tohidi et al. 2019).

1.3 Contribution

A continuous monitoring of the multichannel EEG extremely rises the data dimensions. A real-time EEG signal monitoring is performed by using the wearable sensors and sending these signals to a cloud. Transmission, analysis and storage of such big amount of data are not efficient. Thus, EEG compression plays a crucial role in the current healthcare systems to decrease the cost, consumption, processing time and increase the effectiveness of signal analysis systems. It is essential to diminish the EEG signals dimension while preserving the important diagnostic information in the recorded EEGs (Gu et al. 2018; Elger and Hoppe 2018).

The classical EEG diagnosis systems are based Nyquist theory. They are time-invariant in nature, which results in a worst-case system parameterization (Qaisar 2018, 2019; Qaisar and Subasi 2019b; Budiman 2016; Qaisar et al. 2014; Tan and Jiang 2018). The system computational load and processing activity remain fixed irrespective of the input signal temporal discrepancies. Consequently, they are constrained particularly in the case of intermittent EEG signals. They capture and process a significant number of surplus samples. It augments the overall system computational load, processing and transmission activity and power consumption (Qaisar et al. 2014; Qaisar 2019). These shortfalls can be compensated to a certain extent by using the event-driven analog to digital converters (EDADCs) (Zhang et al. 2017a; Antony et al. 2018; Tohidi et al. 2019; Qaisar et al. 2013; Hou et al. 2018). They adapt the system acquisition and processing activity as a function of the incoming signal variations. It renders a significant computational efficiency of the suggested approach compared to the traditional ones. In this background, original EEG acquisition approaches have been suggested. These solutions are founded on the Level Crossing Sampling Scheme (LCSS) (Qaisar 2018; Qaisar and Subasi 2019b; Zhang et al. 2017a; Antony et al. 2018; Tohidi et al. 2019), and can organize their acquisition rate and conversion resolution in coherence with the incoming signal temporal variations.

In continuation to works devised in Qaisar (2018), Zhang et al. (2017a), Antony et al. (2018), Tohidi et al. (2019), the event-driven acquisition and processing techniques are proposed in this paper. It employs an intelligent emergence of the event-driven signal acquisition and conditioning techniques with robust feature extraction and classification modules. The aim is to contribute in the development of modern computationally efficient EEG diagnosis systems for an effective detection of the epileptic seizers in a cloud environment. The signal is acquired by using an EDADC

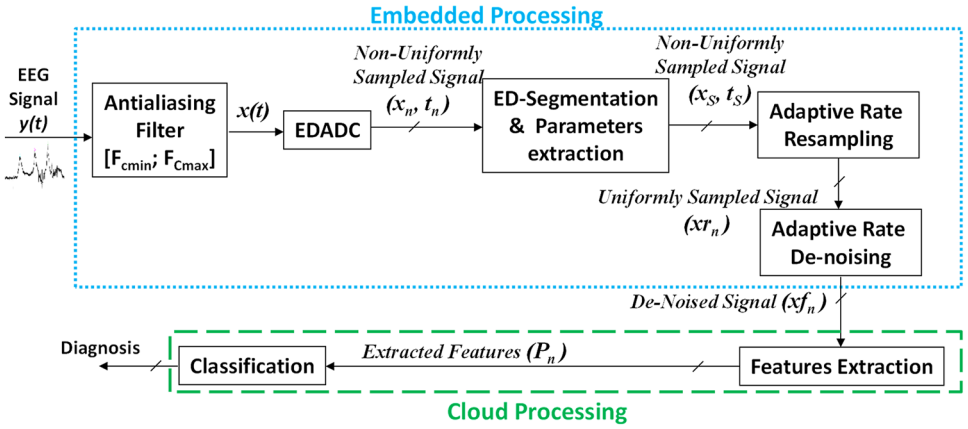

Fig. 1 The proposed system block diagram

to regulate the signal acquisition rate as a function of the input signal variations (Qaisar et al. 2013). It significantly lessens the activity of post processing chain by only acquiring the pertinent information (Qaisar 2018, 2019; Qaisar et al. 2014). The approach is promising and leads towards a proficient front-end electronics along with a real-time data compression.

1.4 Organization

In Sect. 2, information about the proposed event-driven EEG signal acquisition and processing is presented. Besides, EEG data, feature extraction and classification methods are also presented in Sect. 2. Section 3 delivers a complete experimental study of the proposed EEG signal classification framework, where the performances of the proposed acquisition, segmentation, conditioning, features extraction and classification algorithms are evaluated and compared with the classical counterparts. Section 4 discusses the overall system. Conclusion is made in Sect. 5.

2 Materials and methods

In order achieve a real-time compression and to enhance the system processing and transmission efficiencies, an event-driven EEG acquisition and processing framework is suggested which is depicted in Fig. 1. Where, the blue color '….' border is enclosing the processing blocks, embedded in the EEG real-time measuring and processing wearable. The green color '–' border is enclosing the cloud based processing modules.

2.1 The data set

In this study, publicly available (Andrzejak et al. 2001) epileptic seizure EEG dataset[1] is used. Three different classes are studied, normal eyes-open, epileptic ictal, and epileptic interictal (Andrzejak et al. 2001). Each EEG instance is segmented for a time length of 5.898-s and it is acquired with a 12-Bit resolution ADC. The acquisition frequency is 173.61 Hz. Therefore, each digitized instance is composed of 1024 samples.

2.2 The event-driven A/D converter (EDADC)

Figure 1 shows that the incoming EEG signal $y(t)$ is filtered by an analog band-pass filter. The band-limited signal $x(t)$ is acquired with an EDADC. Traditional ADCs are founded on the basis of the Nyquist sampling theory and operates at a unique acquisition frequency. They are parameterized for the worst-case and are ineffective in the case of sporadic EEG signals (Qaisar 2018; Qaisar and Subasi 2019b; Tan and Jiang 2018). This inadequacy is resolved by using EDADCs (Antony et al. 2018; Tohidi et al. 2019; Qaisar et al. 2013; Hou et al. 2018). Their design is based on the Level Crossing Sampling (LCS) (Qaisar et al. 2013). In this case, a sample is acquired when $x(t)$ crosses one of the predefined thresholds. For this reason, sampling frequency is adjusted by the signal. Samples are irregularly spaced in time and the count of samples is proportional the temporal-disparities of $x(t)$.

The signal obtained with LCS is non-uniformly repartitioned in time. Its sampling instants are defined by Eq. (1) (Qaisar 2019). Where, t_n is the current sampling instant, t_{n-1} is the previous one, and the time delay between the current and the previous sampling instants is dt_n(Qaisar 2019). For a given uniform quantization based EDADC its quantum, q,

[1] EEG time series are available under (https://www.meb.unibonn.de/epileptologie/science/physik/eegdata.html).

can be calculated as $q = \frac{\Delta V}{2^{M-1}}$ (Qaisar et al. 2013). Here, ΔV and M are respectively the EDADC dynamics and resolution. The EDADCs acquires only the pertinent EEG information at adaptive-rates. Hence, a diminished number of samples are acquired while comparing with the classical counterparts. It significantly reduces the post processing and transmission Modules activities and realizes power efficient implementations (Qaisar 2018, 2019).

$$t_n = t_{n-1} + dt_n \tag{1}$$

The acquisition principle of an EDADC is different from the classical ADC (Qaisar 2019). While considering the ideal case, for conventional ADCs the sampling instants are accurately known. However, the amplitudes of samples are quantized (Qaisar et al. 2013). Quantization is the only source of error and it depends on the selected ΔV and M (Alickovic and Subasi 2015). It is assessed in terms of the Signal to Noise Ratio (SNR) (Alickovic and Subasi 2015). The SNR is computable as: $SNR_{dB} = 6.02M + 1.76$. It presents an ideal ADC SNR for a full-scale monotonous sinusoidal input and describes its dependency on M. Contrary, amplitudes of samples are ideally known for an EDADC. However, the instants of these samples are quantized according to operating frequency, F_{Timer}, of the timer circuit that is used to record these instants (Qaisar et al. 2013).

The SNR of an ideal EDADC can be calculated as: $SNR_{dB} = -11.19 - 20log\left(f_{sig}.T_{timer}\right)$. Where, f_{sig} is the frequency of full-scale sinusoid, used to evaluate the EDADC. It shows that the SNR of an ideal EDADC is independent of M and it is a function of the f_{sig} and $T_{Timer} = \frac{1}{F_{Timer}}$. A 6.02 dB improvement in the value of SNR is achievable by halving T_{timer} (Qaisar et al. 2013). In this study, a 23-Bit resolution timer is used with F_{Timer}=1 MHz and M=4.

2.3 The event-driven segmentation

The Activity Selection Algorithm (ASA) segments the EDADC output (Qaisar et al. 2014; Qaisar 2019). It employs the sampling process non-uniformity with certain system parameters to select only the pertinent parts of signal. Appealing features of the ASA are not available in the traditional windowing. Only the pertinent signal information is selected. Additionally, the length of window-function is adjusted according to the windowed signal local characteristics (Qaisar et al. 2014; Qaisar 2019). Besides, an effective diminishing of the leakage phenomenon is also attained.

The reference window length L_{ref} is chosen equal to 5.898-s (Qaisar 2019). Qaisar has presented a detailed description of the ASA in Qaisar (2019). It is shown that the ASA adapts the sampling frequency of each selected segment by following the incoming signal variations. It allows adjusting the filter order for each selected segment and contributes in augmenting the system computational efficiency (Qaisar 2019).

2.4 The adaptive rate resampling

The EDADC sampling frequency organizes by following the temporal-disparities of $x(t)$. The maximum sampling frequency, Fs_{max}, of EDADC is defined by Eq. (2) (Qaisar 2019). Where, f_{max} is the $x(t)$ highest frequency component and A_{in} is the input signal amplitude.

$$Fs_{\max} = 2 \cdot f_{\max} \cdot \left(2^M - 1\right) \cdot \frac{A_{in}}{\Delta V}. \tag{2}$$

Let W^i represents the ith selected window, obtained with the ASA. If $Fs^i$is the sampling frequency for W^i, then, it can be calculated as $Fs^i = N^i/L^i$. Here, L^i is the length in seconds and N^i is the number of samples exists in W^i. In order to benefit from the mature signal processing techniques (Tan and Jiang 2018), the W^i is resampled uniformly. The resampling frequency is tuned by following the locally extracted parameters (Qaisar 2019). In this way the selected signal parts are resampled and processed at same or lower rates compared to the traditional counterparts. It results in notable computational gain of the devised method compared to the conventional equals.

If the resampling frequency for $W^i$is Frs^i, then the selection of Frs^i is made in a way that W^i is resampled at inferior or similar rates compared to the conventional equivalents (Qaisar 2019). The process is described in Sect. 2.5. After resampling, there exist Nr^i samples in W^i. The online resampling is attained by using interpolation. The interpolation process alters characteristics of the resampled signal with respect to the original one (Qaisar et al. 2016). Qaisar et al. (2016), shown that for the case of EDADC, the maximum resampling error is bounded by q. However, it could be equal to ΔV in the traditional counterparts. It assures an appropriateness of using simple and low complexity approaches of interpolation in the case of suggested method as compared to the traditional counterparts. Additionally, the focus of this work is to augment the computational efficiency of the EEG wearables and cloud-based computing. For this reason, the Simplified Linear interpolation (*SLI*) is considered for online resampling of the segmented signal parts.

Let xr_n be the nth resampled observation and tr_n is its corresponding instant. If tr_n exists between the non-uniformly sampled signal instants t_{n-1} and t_n. Then the value of xr_n is set equal to the mean of its prior and next non-uniform samples. The highest error per interpolation is limited by $\frac{q}{2}$ (Qaisar et al. 2016).

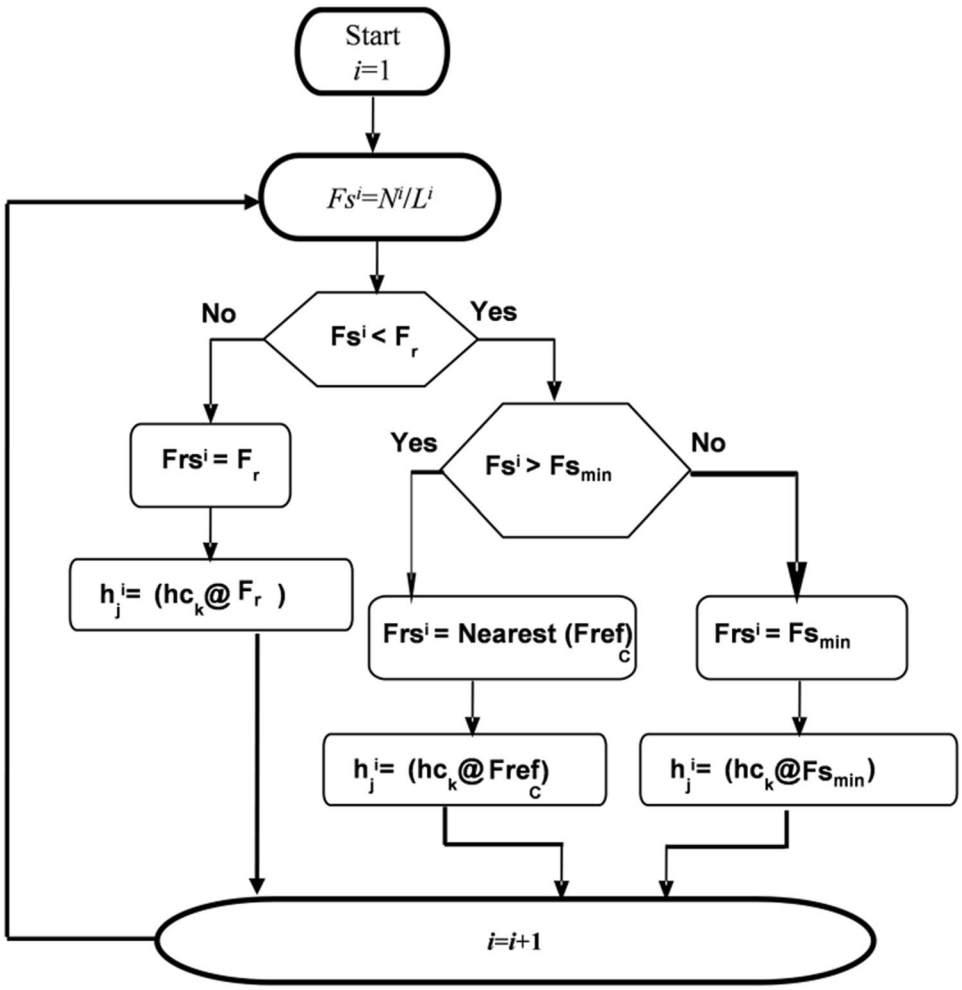

Fig. 2 The ASM chart for choosing Frs^i and a filter from the reference filters bank for W^i

2.5 The adaptive rate denoising

A reference Finite Impulse Response (FIR) filters bank is offline designed for the intended application. The implementation is realized for an appropriate set of parameters while adjusting the reference sampling frequencies *Fref*. Let $[F_{Cmin}; F_{Cmax}]$Hz be the lower and upper cut-off frequencies of the reference band-pass filters. Then, upper bound on *Fref* is selected as F_r, whereas, in order to assure a proper digital filtering operation, the lower bound on *Fref* is chosen as $Fs_{min} \geq 2.F_{Cmax}$ (Tan and Jiang 2018). A uniformly spaced distribution is used for placing different *Fref* elements in the range $[Fs_{min}; F_r]$. If Q is the length of *Fref*, then the procedure of computing *Fref* is mathematically expressed by Eq. (3). The value of Q is always chosen as a binary weighted. In Eq. 4, Δ is a unique offset and can be computed by using Eq. (4).

$$Fref = \left\{Fs_{\min}, Fs_{\min} + \Delta, ..., Fs_{\min} + (Q-1)\Delta = F_r\right\} \tag{3}$$

$$\Delta = \frac{F_r - Fs_{\min}}{Q-1} \tag{4}$$

A suitable filter, from the reference set, is online selected for each W^i. Let h_{c_k} be the selected filter for W^i and is sampled at $Fref_c$. This selection is made on the basis of *Fref* and Fs^i. For a proper filtering, the $Frs^i$and $Fref_c$ should match (Qaisar 2019). In this context, $Frs^i = Fref_c$ is chosen. The process of selecting Frs^i and keeping it coherent with $Fref_c$ is shown in Fig. 2. Where, F_r is the reference sampling frequency. It remains greater than and closer to the Nyquist sampling frequency $F_{Nyq} = 2.f_{max}$.

2.6 The feature extraction

The discriminative features of de-noised signal are extracted by using the Autoregressive (AR) Burg (Alickovic and Subasi 2015). In this case, the xr_n is modeled as an output of a causal, all-pole filter. The process for an *O*thorder model can be expressed by using Eq. (5). Where, xr_n is the input and a_j are the weighing coefficients of the model. b_n is white noise

of variance σ^2. The power spectral density (PSD) of an Oth order model can be estimated by using Eq. (6). Where, F_s is the sampling frequency. In this study, the selective PSD coefficients are used by the post classifiers as discriminative features.

$$z_n = \sum_{j=1}^{O} a_j x r_{n-j} + b_n \tag{5}$$

$$P_{AR \rightleftarrows Burg}(f) = \frac{\sigma^2}{\left|1 + \sum_{j=1}^{O} a_j . e^{\frac{-i2\pi fj}{F_s}}\right|^2} \tag{6}$$

In the implementation of the AR Burg model, we tried several model order parameters to achieve the best performance. The best performance is achieved with a model order of 15.

2.7 The classification methods

Machine learning is a model to address a performance criterion based on training data or historical experiences. It can be used to make predictions or to gain knowledge from the data or for both purposes (Subasi 2019). Artificial Neural Network (ANN) is a set of linked input and output units. Each link can have its specific weight. The learning is accomplished by adjusting these weights. It allows a proper classification of test data. ANN is inherently of parallel nature. Therefore, parallelization approaches can be used to speed up the classification. In the implementation of the ANN, we tried several model parameters such as learning rate, number of neuron hidden layers, activation function and the training algorithm to achieve the best performance. Sigmoid activation function is used in the hidden layer and linear activation function is used in the output layer. Stochastic gradient descent optimizer is used with back propagation. The number of input feature is 64 and the optimum number of nodes in the hidden layer is found 33. The optimum learning rate is 0.7. Support Vector Machine (SVM) conducts the nonlinear mapping to augment the dimensionality of the training data. It allows discovering the most suited classifier which can correctly differentiate among different classes of the testing data. The decision is made on the basis of distance metric. In the implementation of the SVM the Puk kernel with an optimum C value of 100 is utilized. The k-Nearest Neighbors (k-NN) learns and identifies the testing sample by comparing it with training ones. The k Training instances are used to identify the incoming sample. The decision is made on the basis of distance metric. The decision is made on the basis of distance metric, which is Euclidian. In the implementation of the k-NN, the maximum performance is achieved with a k value of 5. The Random Forest is founded on a combination of the tree predictors. Each tree is based on values of an independently sampled random vector. However, a similar distribution is employed for all trees in the forest. The classification error is a function of the accuracy of distinct trees and connotation among them (Subasi 2019). In the implementation of the Random Forest, the maximum performance is achieved with a tree size of 100. The Rotation Forest is an ensemble classifier which prepares a finite number of decision trees. These trees are trained independently by using a dissimilar set of features. The decision trees act as base classifiers. They are subtle to the feature axes rotation. The outcome of rotating features axes is the usage of fewer trees in founding the high accuracy classification regions (Subasi 2019). In the implementation of the Rotation Forest, C.4.5 decision tree is used. The REPTree develops a prediction tree. The absent labels are treated by dividing the given dataset in sections (Subasi 2019). The testing set is identified by using the templates through the added nodes coincidence removing effect (Subasi 2019). In the implementation of the REPTree default parameters are used. The C4.5 decision tree is an evolution of the algorithm, originally suggested by the Ross Quinlan (Subasi 2019). It generates decision trees which are afterwards employed for the classification. In beginning the tree root is decided. Afterwards, the property, precised by the node, is experienced. It allows digging down the tree in relation to a given instance of the attribute value. This process continues until it comes upon a leaf. Finally, the under test instances are labelled by using characteristics of leaves (Subasi 2019). In the implementation of the C4.5 default parameters are used. The NBTree is an extension of the Naive Bayes classifier (Subasi 2019). It uses the training set, composed of a finite number of sets of the labeled instances, to create a decision tree with Naive Bayes category. The classification process starts with deciding the tree root. In next step, the quality described by the node is used for propagating down the tree. At last, the test instances are classified by using characteristics of Naïve Bayes category leaves (Subasi 2019). In the implementation of the NBTree, the default parameters are used. The RandomTree is an ensemble of predictors. Its classification principle is to pass the input variants to a collection of predictors. The classification vote of each predictor is employed to make the final decision. The label of the class is decided on the base of majority of votes. In the implementation of the RandomTree, the default parameters are used. CART is one of the most well-known and successful methods among the decision tree induction. Since it is nonparametric algorithm and works to form binary trees using the data described by discrete and continuous features. Searching for the best separations with the reduction criterion of impurity is known as the Gini index. It is feasible to make use of some impurity measure or entropy instead of using the Gini index. For each split,

Breiman et al. (1998), proposed an efficient way to identify the strong optimal classes. In the implementation of the CART, the default parameters are used. Logical Analysis of Data (LAD) tree makes use of a classifier based on learning for the binary target variable. In this technique, a logical expression is there that can be used to make a differentiation between the negative and positive data set samples. The selection of a subset of large set patterns and the generation of large set patterns are required for construction of the LAD model for any data set The boosting algorithm is used for the LAD Tree learning algorithm with the purpose to create a substitute decision tree (Holmes et al. 2002). In the implementation of the LADTree, the default parameters are used. All classifiers are implemented in WEKA.[2]

2.8 Performance evaluation metrics

2.8.1 A.*Compression gain*

One metric is to evaluate the system performance in terms of compression gain. In classical case, $x(t)$ is acquired at a fixed rate. Therefore, the total count of samples for a considered time length L_T is straightforward to compute. Let F_r be the selected sampling frequency for the acquisition of the EEG Signals. Then, the acquired number of samples N for the considered L_T can be calculated as $N = F_{ref} \times L_T$.

For the EDADC, the sampling frequency is not unique, and it adapts as a function of the input signal temporal variations (Qaisar 2018). Therefore, for a considered time length $L_T$the acquired number of samples can be different. Let N_{ED} is the number of samples obtained in the devised solution. Then the compression gain, G_{COMP}, can be calculated by using Eq. (7).

$$G_{COMP} = \frac{N}{N_{ED}} \tag{7}$$

2.8.2 B. Computational complexity

In this paper, computational complexity of the embedded processing modules is studied in detail. The complexity of cloud processing modules is analyzed at an abstract level by considering the compression gain of the proposed approach. The resampled signal is de-noised by using an enhanced adaptive rate FIR (*ARFIR*) filtering tactic (Qaisar 2019). The arithmetic complexity of a classical K order FIR filter is well known. It executes K additions and K multiplications while calculating an output sample. Therefore, for N samples the entire computational complexity C_{FIR} can be calculated by using Eq. (8).

$$C_{FIR} = \underbrace{K.N}_{Additions} + \underbrace{K.N}_{Multiplications} \tag{8}$$

For the case of devised solution, the online system adaptation needs additional operations. Firstly, a reference filter hc_k is selected for W^i. It requires $\log_2(Q)$ comparisons for the worst case. Here, Q is the binary weighted count of the frequencies in *Fref*. Secondly the selected windows are resampled uniformly.

The resampling is realized by using the *SLI*. For W^i, the complexity of this procedure is Nr^i additions and Nr^i binary weighted right shifts. The complexity of binary weighted right shift is negligible compared to the addition and multiplication processes (Cavanagh 2017). For this reason, the computational complexity of *SLI* for W^i is estimated as Nr^i additions.

After resampling, a K^i order filter performs $K^i.Nr^i$ multiplications and $K^i.\ Nr^i$ additions for W^i. In order to keep the complexity of proposed *ARFIR* comparable with the classical one, the arithmetic cost of a comparison is considered equal to that of an addition. In this framework, the computational complexities of the *ARFIR* is presented by Eq. (9).

$$C_{ARFIR} = \underbrace{K^i.Nr^i + Nr^i + \log_2(Q)}_{Additions} + \underbrace{K^i.Nr^i}_{Multiplications} \tag{9}$$

2.8.3 C. Classification performance

The de-noised signal discriminative parameters are extracted by using the *AR Burg* method. These extracted parameters are employed by several robust classification algorithms in order to classify the EEG signals. The performance of whole chain is studied in terms of the classification performance. The limited dataset causes difficulties in estimating the classification performances. In this context, the cross-validation schema is frequently used (Subasi 2019). Hence, the tenfold cross-validation is utilized in this study. Total classification accuracy is used to measure the performances of employed models.

3 Experimental results

The performance of suggested solution is studied for EEG signals, obtained from the EEG epilepsy database (Andrzejak et al. 2001).Frequency range of the EEG signals is between [0; 85] Hz (Tsipouras 2019). The signal is acquired with traditional ADC of 12-Bit resolution and at a sampling frequency of 173.61 Hz (Andrzejak et al. 2001).

[2] https://www.cs.waikato.ac.nz/ml/weka/.

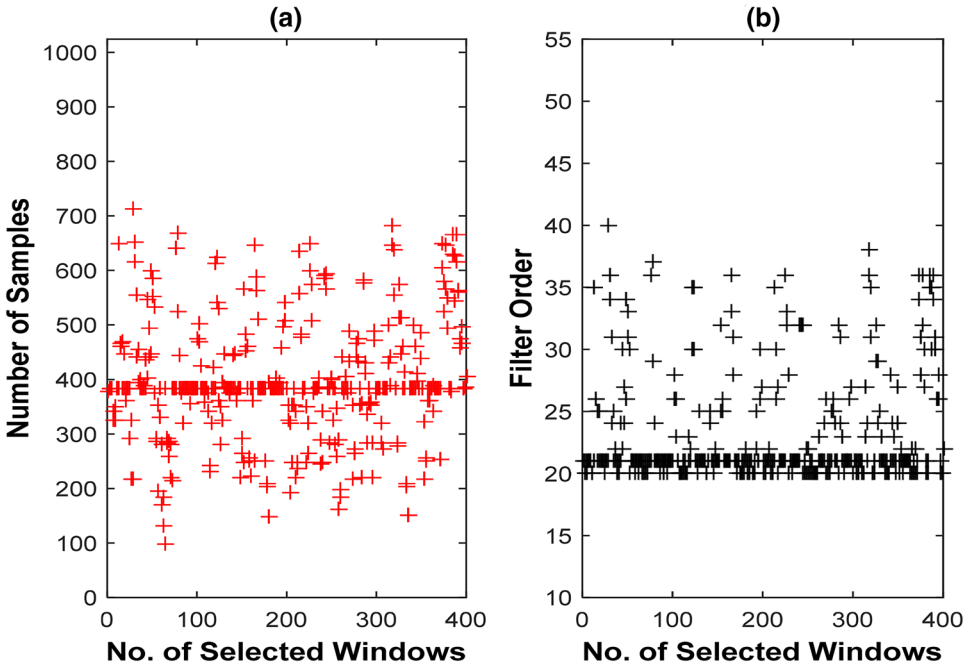

Fig. 3 The number of samples per window versus number of windows for class epileptic ictal (**a**), the filter orders versus number of windows obtained for class epileptic ictal (**b**)

In this study, each EEG instance is segmented for a time length of 5.898-s. Three different categories of EEG signals are considered. These are normal eyes open, epileptic ictal and epileptic interictal (Andrzejak et al. 2001). Total 1200 EEG instances are considered. In order to achieve an equal representation, 400 instances are considered for each class.

In the classical case, for the selected time length of 5.898-s and sampling frequency of 173.61 Hz, each instance is composed of 1024 samples. According to Andrzejak et al. (2001), for the devised solution, the $y(t)$ is passed through a band-pass filter of $[F_{Cmin}=0.5;\ F_{Cmax}=40]$Hz to obtain $x(t)$. The $x(t)$ is acquired with an EDADC of $M=4$. Since the EEG signals are band limited by $f_{max}=40$ Hz, the maximum EDADC sampling frequency for a full-scale EEG signal is $Fs_{max}=1.2$ kHz (cf. Equation 2).

The EDADC output is segmented by using the ASA. The reference window length L_{ref} is chosen equal to 5.898-s (Qaisar 2019). The ASA adapts Frs^i by following the incoming signal variations. It allows adjusting the filter order K^i for each W^i and contributes in augmenting the system computational efficiency (Qaisar 2019). To illustrate this process, number of samples, Nr^i, and filter orders, K^i, for all selected windows for the epileptic ictal class are shown in Fig. 3.

Figure 3a shows that the EDADC and the ASA allow adjusting the resampling frequency, Frs^i, by adapting the length, L^i, and number of samples, N^i, for each W^i by following the $x(t)$ variations (Qaisar 2019). It allows focusing only on the interesting signal parts and achieves a reduced number of samples for each instance compared to the classical one. On other hand, in the case of traditional counterparts, the window length and the count of samples per instance remain unique, 5.898-s and 1024 samples respectively, in spite of the incoming signal disparities. It causes a surplus augmentation of processing and power consumption as compared to the suggested solution.

The compression gains for all 400 instances of each class are computed by using Eq. (7). These are respectively 2.5, 4.8, and 2.6 folds for epileptic ictal, epileptic interictal, and normal eyes open. The overall attained average compression gain for all three classes is 3.3 times.

The output of ASA is uniformly resampled by employing the SLI. The resampled signal is de-noised by using an ARFIR filtering technique (Qaisar 2019). Frequencies higher than 30 Hz mainly present low energy noise and can be eliminated for effective epilepsy detection. In this framework, a band-pass filters bank is offline designed. Each filter is designed for the cut-off frequencies of $[F_{Cmin}=0.5;\ F_{Cmax}=30]$Hz. It allows focusing on the relevant EEG band while attenuating the unwanted noise (Tsipouras 2019). It results in an improved accuracy of the post features extraction and classification modules. The filters bank is designed for a set of sampling frequencies, $Fref$, between $Fs_{min}=65.5$ Hz $\geq 2.F_{Cmax}$ to $F_r=174$ Hz. In this case $\Delta=3.5$ Hz is chosen. It realizes a bank of $Q=32$ band-pass FIR filters. A summary of the employed filters bank is presented in Table 1. It illustrates that how the increase in sampling frequency results into a higher order filters and vice versa. For the selected specification the lowest order filter 20th order, in the bank is obtained for $Fref_1=Fs_{min}=65.5$ Hz and the highest order filter, 56th order, in the bank is obtained for $Fref_{32}=F_r=174$ Hz.

Table 1 Summary of the reference filters bank parameters

hc_k	$h1_k$	$h2_k$	$h3_k$	$h4_k$	$h5_k$	$h6_k$	$h7_k$	$h8_k$	$h9_k$	$h10_k$	$h11_k$	$h12_k$	$h13_k$	$h14_k$	$h15_k$	$h16_k$
$Fref_c$(Hz)	65.5	69	72.5	76	79.5	83	86.5	90	93.5	97	100.5	104	107.5	111	114.5	118
K^i	20	21	22	24	25	26	27	28	30	31	32	33	34	36	37	38
hc_k	$h17_k$	$h18_k$	$h19_k$	$h20_k$	$h21_k$	$h22_k$	$h23_k$	$h24_k$	$h25_k$	$h26_k$	$h27_k$	$h28_k$	$h29_k$	$h30_k$	$h31_k$	$h32_k$
$Fref_c$(Hz)	121.5	125	128.5	132	135.5	139	142.5	146	149.5	153	156.5	160	163.5	167	170.5	174
K^i	39	40	41	43	44	45	46	47	48	49	51	52	53	54	55	56

Table 2 The summary of computational gain of ARFIR over classical filtering

CLASS	Gain in additions (*ARFIR*)	Gain in multiplications (*ARFIR*)
Epileptic ictal	7.16	7.51
Epileptic interictal	8.78	9.23
Normal eyes open	7.20	7.56

The resampling frequency, Frs^i, can be specific for each W^i and it is kept coherent with the sampling frequency, $Fref_c$, of online chosen reference filter, hc_k. It is realized by using the ASM, shown in Fig. 2. The filtering process enhances the intended signal SNR (Signal to Noise Ratio) and allows achieving a better classification performance (Subasi 2019; Tsipouras 2019). The online filter adaption, is clear from Fig. 3b. It allows achieving the signal denoising with a reduced arithmetic cost compared to the counter time invariant traditional methods (Qaisar 2019).

The computational gain of the proposed *ARFIR* is computed over the classical one by using Eqs. (8), and (9). Results are outlined in Table 2. It illustrates that the proposed *ARFIR* technique achieves noticeable computational gains over the traditional counterpart. It is achieved by intelligently adapting the system parameters like Frs^i, Nr^i and K^i for each W^i. These variations are piloted by the incoming signal.

The average gain for all the intended three class is also computed. The gain in additions and multiplications for the *ARFIR* is 7.71 and 8.10 times respectively.

The discriminative features of the denoised signals are extracted with the *AR Burg*. Afterwards, these features are used by the classifiers in order to automatically diagnose the cardiac arrhythmia. A summary of results, obtained by using different classifiers for the intended EEG signals, for the classical and the suggested methods, are respectively outlined in Tables 3 and 4.

The processing performance of the suggested methods over the classical counterpart is demonstrated with the help of results, outlined in Table 2. However, while assuring a remarkable processing gain, the proposed approaches might suffer in terms of the classification performance. Nevertheless, Tables 3 and 4 show that the classification accuracies achieved with the proposed solution are of high precision and satisfactory.

Table 3 The Classification accuracies for three-class EEG dataset, (classical case)

	Normal	Ictal	Interictal	Average
SVM	1	0.973	0.975	0.983
k-NN	1	0.978	0.975	0.984
ANN	1	0.985	0.97	0.985
Random Forest	1	0.965	0.985	0.983
CART	0.968	0.933	0.965	0.955
C4.5	0.98	0.95	0.965	0.965
Rotation Forest	1	0.973	0.983	0.985
REPTree	0.953	0.91	0.97	0.944
Random Tree	0.968	0.948	0.958	0.958
LADTree	0.97	0.938	0.963	0.957
NBTree	0.958	0.923	0.953	0.944

Table 4 The Classification accuracies for three-class EEG dataset, (proposed case)

	Normal	Ictal	Interictal	Average
SVM	0.968	0.785	0.973	0.908
k-NN	0.92	0.848	0.953	0.907
ANN	0.95	0.948	0.948	0.948
Random Forest	0.975	0.945	0.973	0.964
CART	0.92	0.893	0.963	0.925
C4.5	0.93	0.913	0.948	0.93
Rotation Forest	0.965	0.95	0.975	0.963
REPTree	0.92	0.873	0.94	0.911
Random Tree	0.938	0.86	0.963	0.92
LADTree	0.93	0.883	0.938	0.917
NBTree	0.895	0.855	0.923	0.891

Table 3 shows that the best average classification accuracy, achieved for the classical counterpart, is 98.5%. It is achieved with the Rotation Forest and ANN.

Table 4 shows that for the proposed method while solely looking at the level of each class, the highest accuracy is achieved for the Epileptic Interictal class. The accuracy of 97.5% is attained by the Rotation Forest and the Random Forest followed with an accuracy of 97.3%.

The average classification accuracies, obtained for the three-class EEG dataset, in the case of SVM, k-NN, ANN, CART, C4.5, REPTree, RandomTree, LADTree, Random Forest, and Rotation Forest are above 90.7%. The highest average classification accuracy of 96.4% is obtained with RandomForest and Rotation Forest followed with an average classification accuracy of 96.3%. The lowest, accuracy of 89.1% is obtained with the NBTree for the studied case.

4 Discussion

4.1 Comparison with classical counterpart

The appealing features of the suggested event-driven solution are clear from Tables 2, 3, 4 and Fig. 3. It is attained by smartly attaining the adaptive rate signal processing. The adaptive feature of ASA is depicted with values of Nr^i. It shows that how the Frs^i is adjusted as a function of activity which exists in W^i. It confirms the capability of devised system to adjust its acquisition rate as a function of the input signal variations. The adaptation of $Frs^i$and Nr^i also illustrates the evading of needless interpolations during the resampling process. K^i represents that how the adjustment of hc_k for W^i avoids the unnecessary operations to deliver the filtered signal. It yields a noteworthy computational gain of the proposed *ARFIR* methods over the traditional counterparts (Qaisar et al. 2014; Qaisar 2019).The overall gains in additions and multiplications for the ARFIR over the classical approach are 7.71 and 8.10 folds respectively. Additionally, the system attains an overall compression gain of 3.3 times over the classical counterpart. It assures a noticeable reduction in the activity of post processing, transmission and analysis modules. As a result, the data transmission bandwidth requirements are also diminished by more than 70% as compared to the traditional approach. In addition, the signal is digitized with a 4-Bit resolution EDADC. In the classical case, the digitization is performed with an 16-Bit resolution ADC. It confirms a simpler circuit level realization compared to the counterparts. On the side of cloud processing, the denoised signal features are extracted with the AR Burg. The processing of 3.3 times less number of samples with the reduced order AR Burg models assure a more than 70% processing load diminishing compared to the counter classical approach. Consequently, it confirms that the integration of designed solution can potentially augment the effectiveness of modern cloud based mobile healthcare systems.

The highest accuracy, achieved with the designed system, is 2.1% less than the highest classification accuracy of the classical counterpart. It shows that the proposed solution attains comparable classification accuracy as compared to the classical counterpart while attaining a noticeable processing, transmission and hardware simplicity gain over it.

4.2 Comparison with state-of-the-art

The idea of embedding the event-driven signal acquisition and processing in the automatic epileptic seizure detection systems is quite a novel approach. In Qaisar (2018), Zhang et al. (2017a), Antony et al. (2018) and Tohidi et al. (2019) novel approaches have been proposed for an effective EEG acquisition. These solutions are mainly focusing on the adaptive-rate A/D conversion of the EEG signal and are founded on the basis of LCS (Qaisar et al. 2013). In Qaisar (2018) and Antony et al. (2018), authors have demonstrated that how the usage of LCSS based architecture leads towards a simplified and power efficient architectures. In Qaisar (2018), Qaisar has shown that how the system can adjust its processing activity as a function of the input signal variations. It resulted in notable compression gain compared to the counter equals.

In contrast to Zhang et al. (2017a), Antony et al. (2018) and Tohidi et al. (2019) the proposed solution is not only dealing with the design of an effective EDADC for the EEG signal acquisition but additionally it presents the application of ASA, adaptive-rate resampling, denoising, features extraction and classification approaches on the EDADC output. An effective segmentation and conditioning of the digitized EEG signals is realized to well prepare them for the post analysis and classification modules. Furthermore, the denoised EEG signals are proficiently analyzed and classified to achieve a completely automatic EEG monitoring and diagnosis system.

The suggested approach is quite novel. It is not straightforward to compare the proposed approach with the state-of-the-art, solutions, since they are based on the conventional Nyquist sampling and processing based approaches. Additionally, each study uses different number of subjects, different types of epilepsy study can be subject dependent or independent. It is also tricky to compare the diversity of classification methods and techniques for EEG signal processing. However, a comparison is described among the key previous studies that use the same EEG dataset (Andrzejak et al. 2001). The accuracy of classification for all considered studies are compared and presented in Table 5. It shows that the success rate of the technique which we have employed is comparable to the success rate of others (Rizal and Hadiyoso 2018; Li et al. 2018; Tanveer et al. 2018; Sharma et al. 2017; Mert and Akan 2018).

Table 5 Comparison with previous studies

Study	Classification method	Features extraction	Accuracy (%)
(Rizal and Hadiyoso 2018)	SVM	Multi-Distance Signal Level Difference (MSLD)	97.70
(Li et al. 2018)	Quadratic Discriminant (QD)	Entropy Analysis	92.80
(Tanveer et al. 2018)	Twin SVM (TSVM), Least Squares TSVM (LS-TSVM)	Flexible Analytic Wavelet Transform (FAWT) and Hjorth parameters	98.33
(Sharma et al. 2017)	Least Squares SVM (LSSVM)	Flexible Analytic Wavelet Transform (FAWT) with fractal dimension	98.67
(Mert and Akan 2018)	Energy distribution Identifier of the Intrinsic Mode Functions (IMFs)	Empirical Mode Decomposition (EMD) and IMFs	97.89
(Singh and Malhotra 2019)	Random Forest	Fast Walsh Hadamard transform and higher order spectra (HOS)	99.40
(Anupallavi and MohanBabu 2020)	SVM	Bi-Spectral Phase Concurrence Index (BSPCI)	98.79
(Nishad and Pachori 2020)	Random Forest	Tunable-Q Wavelet Transform (TQWT)	99.00
This study	Rotation Forest	SLIN + AR Burg	97.50

In Rizal and Hadiyoso (2018) authors have used the sample entropy on the Multi-Distance Signal Level Difference (MSLD) for features extraction and the classification is realized by utilizing the SVM algorithm. The highest classification accuracy of 97% is reported. In Li et al. (2018) authors have employed the entropy analysis for the extraction of features. The classification is realized with the Quadratic Discriminant (QD) algorithm. The highest classification accuracy of 92.8% is reported. In Tanveer et al. (2018) the extraction of features is realized with the flexible analytic wavelet. The classification is carried out with the Twin SVM (TSVM) algorithm. The highest classification accuracy of 98.33% is reported. In Sharma et al. (2017) the extraction of features is realized with flexible analytic wavelet transform (FAWT) with fractal dimension. The classification is carried out with the Least Squares SVM (LSSVM) algorithm. The highest classification accuracy of 98.67% is reported. In Mert and Akan (2018) the extraction of features is realized with the Empirical Mode Decomposition (EMD) and the Intrinsic Mode Functions (IMFs). The classification is carried out with the energy distribution identifier of the IMFs. The highest classification accuracy of 97.89% is reported. In Singh and Malhotra (2019) the extraction of features is realized with the Fast Walsh Hadamard transform and Higher Order Spectra (HOS). The classification is carried out with the Random Forest algorithm. The highest classification accuracy of 99.4% is reported. In Anupallavi and MohanBabu (2020) the extraction of features is realized with the Bi-Spectral Phase Concurrence Index (BSPCI). The classification is carried out with the SVM. The highest classification accuracy of 98.79% is reported. In Nishad and Pachori (2020) the extraction of features is realized with the Tunable-Q Wavelet Transform (TQWT). The classification is carried out with the Random Forst. The highest classification accuracy of 99% is reported. In Nishad and Pachori (2020) the extraction of features is realized with the Tunable-Q Wavelet Transform (TQWT). The classification is carried out with the Random Forst. The highest classification accuracy of 99% is reported.

In this study, the ARFIR, the AR Burg and the Rotation Forest achieved the best classification accuracy of 97.50%. The highest average accuracy for three-class EEG signals is 96.4%. The average accuracy of the suggested framework is 2.1% less than the conventional equal (cf. Tables 3 and 4). The accuracy of suggested framework is higher than the method presented in Li et al. (2018). The precision is quite comparable with Rizal and Hadiyoso (2018) and Mert and Akan (2018). The accuracy is a bit less than the methods reported in Tanveer et al. (2018), Sharma et al. (2017), Singh and Malhotra (2019), Anupallavi and MohanBabu (2020) and Nishad and Pachori (2020).

The key improvement of the suggested framework over the previous ones is to eliminate the redundant samples and introduce a real-time compression gain. It is accomplished by intelligently embedding the event-driven acquisition and segmentation tools in the system. The proposed architecture has achieved 3.3 times compression gain. It introduced a substantial computational complexity decrease during the post processing modules. The performance of adaptive rate filtering based denoising module over the counter traditional one is validated. The overall gains in additions and multiplications for the ARFIR over the classical approach are 7.71 and 8.10 folds respectively. Furthermore, in the designed method, the denoised signal features are extracted with the AR Burg. The processing of 3.3 fold less number of samples with the lowered order AR Burg models assure a more than 70% processing load decrease compared to the conventional counterparts.

It is also demonstrated that the developed solution achieves high classification accuracy, comparable with the classical acquisition and processing-based solutions, while ensuring a significant computational gain.

5 Conclusion

An innovative event-driven Electroencephalogram signal acquisition, processing and classification method is developed for the cloud based mobile health monitoring. It is revealed that the designed method eliminates the redundant samples to process. The developed framework achieves a 3.3 times compression gain. It achieved a significant reduction in the computational complexity of developed framework compared to the conventional counterparts. The overall gains in additions and multiplications for the adaptive-rate filtering over the conventional approach are 7.71 and 8.10 folds respectively. The attained compression gain also confirms a significant diminishing in terms of the signal transmission between EEG wearable and the cloud-based processing and classification module. Furthermore, a similar amount of processing gain is also assured by the post cloud based features extraction and classification modules, since they have to deal with more than 70% lesser data points compared to the classical counterpart.

The best classification accuracies of 97.5% and 96.4% are secured for the mono-class and the average three-class identification. It is revealed that the proposed method achieves a similar classification performance compared to the classical counterpart while realizing a remarkable processing and transmission bandwidth gain over it. Furthermore, the precision of designed method is also comparable with the state-of-the-art counter ones. It proves the benefit of utilizing the proposed solution for the design and development of effective and low power EEG wearables.

The developed framework can also be utilized by the medical practitioners in order to accomplish an augmented diagnosis. Additionally, the performance of developed framework based on the nature of employed interpolator, denoising stage, parameters extraction module and the classification algorithm. A study on the developed framework performance whereas utilizing the polynomial or spline interpolators and ensemble classifiers is a future work.

Acknowledgement Authors are thankful to anonymous reviewers for their valuable feedback.

Funding This project is funded by the Effat University with the decision number UC#7/28Feb 2018/10.2-44i.

Compliance with ethical standards

Conflicts of interest Authors declare no conflict of interest.

Ethical approval This article does not contain any studies with human participants or animals performed by any of the authors.

References

Alickovic E, Subasi A (2015) Effect of multiscale PCA de-noising in ECG beat classification for diagnosis of cardiovascular diseases. Circ Syst Signal Process 34(2):513–533

Andrzejak RG, Lehnertz K, Mormann F, Rieke C, David P, Elger CE (2001) Indications of nonlinear deterministic and finite-dimensional structures in time series of brain electrical activity: dependence on recording region and brain state. Phys Rev E 64(6):061907

Antony A, Paulson SR, Moni DJ (2018) Asynchronous level crossing ADC design for wearable devices: a review. Int J Appl Eng Res 13(4):1858–1865

Anupallavi S, MohanBabu G (2020) A novel approach based on BSPCI for quantifying functional connectivity pattern of the brain's region for the classification of epileptic seizure. J Ambient Intell Human Comput. https://doi.org/10.1007/s12652-020-01774-w

Baskar K, Karthikeyan C (2019) Epilepsy seizure detection using akima spline interpolation based ensemble empirical mode Kalman filter decomposition by EEG signals. J Med Imaging Health Inf 9(6):1320–1328

Bayrakdar ME (2019a) Priority based health data monitoring with IEEE 80211 af technology in wireless medical sensor networks. Med Biol Eng Comput 57(12):2757–2769

Bayrakdar ME (2019b) Fuzzy logic based coordinator node selection approach in wireless medical sensor networks. In: 2019 4th International conference on computer science and engineering (UBMK), Turkey. IEEE, pp 340–343

Breiman L, Friedman J, Olshen R, Stone C (1998) Classification and regression trees Boca Raton, chap. 4. CRC, Boca Raton

Budiman ES (2016) Multi-rate analyte sensor data collection with sample rate configurable signal processing. US Patent 9,474,475

Cavanagh J (2017) Computer arithmetic and Verilog HDL fundamentals. CRC Press, USA

Chen G, Xie W, Bui TD, Krzyżak A (2017) Automatic epileptic seizure detection in EEG using nonsubsampled wavelet–fourier features. J Med Biol Eng 37(1):123–131

Correa AG, Orosco LL, Diez P, Leber EL (2019) Adaptive filtering for epileptic event detection in the EEG. J Med Biol Eng 39(6):912–918

Devinsky O, Friedman D, Cheng JY, Moffatt E, Kim A, Tseng ZH (2017) Underestimation of sudden deaths among patients with seizures and epilepsy. Neurology 89(9):886–892

Elger CE, Hoppe C (2018) Diagnostic challenges in epilepsy: seizure under-reporting and seizure detection. Lancet Neurol 17(3):279–288

Gu Y, Cleeren E, Dan J, Claes K, Van Paesschen W, Van Huffel S, Hunyadi B (2018) Comparison between scalp EEG and behind-the-ear EEG for development of a wearable seizure detection system for patients with focal epilepsy. Sensors 18(1):29

Gupta V, Pachori RB (2019) Epileptic seizure identification using entropy of FBSE based EEG rhythms. Biomed Signal Process Control 53:101569

Holmes G, Pfahringer B, Kirkby R, Frank E, Hall M (2002) Multiclass alternating decision trees. In: European conference on machine learning. Springer, Berlin, Heidelberg, pp 161–172

Hosseini MP, Soltanian-Zadeh H, Elisevich K, Pompili D (2016) Cloud-based deep learning of big EEG data for epileptic seizure prediction. In: 2016 IEEE global conference on signal and

information processing (GlobalSIP), Washington, USA. IEEE, pp 1151–1155
Hou Y, Qu J, Tian Z, Atef M, Yousef K, Lian Y, Wang G (2018) A 61-nW level-crossing ADC with adaptive sampling for biomedical applications. IEEE Trans Circuits Syst II Express Briefs 66(1):56–60
Li P, Karmakar C, Yearwood J, Venkatesh S, Palaniswami M, Liu C (2018) Detection of epileptic seizure based on entropy analysis of short-term EEG. PLoS One 13(3):e0193691. https://doi.org/10.1371/journal.pone.0193691
Martinez-del-Rincon J, Santofimia MJ, del Toro X, Barba J, Romero F, Navas P, Lopez JC (2017) Non-linear classifiers applied to EEG analysis for epilepsy seizure detection. Expert Syst Appl 86:99–112
Mert A, Akan A (2018) Seizure onset detection based on frequency domain metric of empirical mode decomposition. SIViP 12(8):1489–1496
Mesin L (2016) A neural algorithm for the non-uniform and adaptive sampling of biomedical data. Comput Biol Med 71:223–230
Nishad A, Pachori RB (2020) Classification of epileptic electroencephalogram signals using tunable-Q wavelet transform based filterbank. J Ambient Intell Human Comput. https://doi.org/10.1007/s12652-020-01722-8
Osorio I, Frei MG (2017) Algorithm for detecting a seizure from cardiac data. US Patent 9,700,256
Pitkänen A, Buckmaster P, Galanopoulou AS, Moshé SL (2017) Models of seizures and epilepsy. Academic Press, USA
Qaisar SM (2018) A computationally efficient EEG signals segmentation and de-noising based on an adaptive rate acquisition and processing. In: 2018 IEEE 3rd International conference on signal and image processing (ICSIP), Shenzhen, China. IEEE, pp 182–186
Qaisar SM (2019) Efficient mobile systems based on adaptive rate signal processing. Comput Electr Eng 79:106462
Qaisar SM, Subasi A (2019a) Efficient epileptic seizure detection based on the event driven processing. Procedia Comput Sci 163:30–34
Qaisar SM, Subasi A (2019b) Adaptive rate EEG signal processing for epileptic seizure detection. In: 2019 13th international conference on sampling theory and applications (SampTA), Bordeaux, France. IEEE, pp 1–3
Qaisar SM, Yahiaoui R, Gharbi T (2013) An efficient signal acquisition with an adaptive rate A/D conversion. In: 2013 IEEE international conference on circuits and systems (ICCAS), Kuala Lumpur, Malaysia. IEEE, pp 124–129
Qaisar SM, Fesquet L, Renaudin M (2014) Adaptive rate filtering a computationally efficient signal processing approach. Signal Process 94:620–630
Qaisar SM, Akbar M, Beyrouthy T, Al-Habib W, Asmatulah M (2016) An error measurement for resampled level crossing signal. In: 2016Second international conference on event-based control, communication, and signal processing (EBCCSP), Krakow, Poland. IEEE, pp 1–4
Rizal A, Hadiyoso S (2018) Sample entropy on multidistance signal level difference for epileptic EEG classification. Sci World J 2018:8463256. https://doi.org/10.1155/2018/8463256
Saxena S, Li S (2017) Defeating epilepsy: a global public health commitment. Epilepsia Open 2(2):153–155
Schmidt D, Sillanpää M (2016) Prevention of epilepsy: issues and innovations. Curr Neurol Neurosci Rep 16(11):95
Schröder AL, Ombao H (2019) FreSpeD: Frequency-specific change-point detection in epileptic seizure multi-channel EEG data. J Am Stat Assoc 114(525):115–128
Sharma M, Pachori RB, Acharya UR (2017) A new approach to characterize epileptic seizures using analytic time-frequency flexible wavelet transform and fractal dimension. Pattern Recogn Lett 94:172–179
Sharma M, Bhurane AA, Acharya UR (2018) MMSFL-OWFB: a novel class of orthogonal wavelet filters for epileptic seizure detection. Knowl-Based Syst 160:265–277
Singh K, Malhotra J (2019) IoT and cloud computing based automatic epileptic seizure detection using HOS features based random forest classification. J Ambient Intell Hum Comput. https://doi.org/10.1007/s12652-019-01613-7
Subasi A (2019) Practical guide for biomedical signals analysis using machine learning techniques: A MATLAB based approach. Academic Press, USA
Tan L, Jiang J (2018) Digital signal processing: Fundamentals and applications. Academic Press, USA
Tanveer M, Pachori RB, Angami NV (2018) Classification of seizure and seizure-free EEG signals using Hjorth parameters. In: 2018 IEEE symposium series on computational intelligence (SSCI), India. IEEE, pp 2180–2185
Tawfik NS, Youssef SM, Kholief M (2016) A hybrid automated detection of epileptic seizures in EEG records. Comput Electr Eng 53:177–190
Tohidi M, Madsen JK, Moradi F (2019) Low-power high-input-impedance EEG signal acquisition SoC with fully integrated IA and signal-specific ADC for wearable applications. IEEE Trans Biomed Circuits Syst 13(6):1437–1450
Tsipouras MG (2019) Spectral information of EEG signals with respect to epilepsy classification. EURASIP J Adv Signal Process 2019(1):10
Zazzaro G, Cuomo S, Martone A, Montaquila RV, Toraldo G, Pavone L (2019) EEG signal analysis for epileptic seizures detection by applying data mining techniques. Internet Things. https://doi.org/10.1016/j.iot.2019.03.002
Zeng K, Yan J, Wang Y, Sik A, Ouyang G, Li X (2016) Automatic detection of absence seizures with compressive sensing EEG. Neurocomputing 171:497–502
Zhang X, Li J, Liu Y, Zhang Z, Wang Z, Luo D, Zhou X, Zhu M, Salman W, Hu G (2017a) Design of a fatigue detection system for high-speed trains based on driver vigilance using a wireless wearable EEG. Sensors 17(3):486
Zhang Y, Liu B, Ji X, Huang D (2017b) Classification of EEG signals based on autoregressive model and wavelet packet decomposition. Neural Process Lett 45(2):365–378